Rock and Soil Mechanics

Volume 41 | Issue 7 Article 5

12-22-2020

An elastoplastic model for energy soils considering filling and bonding effects

Qing-meng YUAN
School of Civil Engineering, Qingdao University of Technology, Qingdao, Shandong 266033, China

Liang KONG
School of Science, Qingdao University of Technology, Qingdao, Shandong 266033, China,
qdkongliang@163.com

Ya-peng ZHAO
School of Civil Engineering, Qingdao University of Technology, Qingdao, Shandong 266033, China

Rock and Soil Mechanics 2020 41(7): 2304−2312 ISSN 1000−7598
https: //doi.org/10.16285/j.rsm.2019.7115 rocksoilmech.researchcommons.org/journal

An elastoplastic model for energy soils considering filling and bonding effects

YUAN Qing-meng[1], KONG Liang[1, 2], ZHAO Ya-peng[1]

1. School of Civil Engineering, Qingdao University of Technology, Qingdao, Shandong 266033, China
2. School of Science, Qingdao University of Technology, Qingdao, Shandong 266033, China

Abstract: The filling and bonding effects of hydrate increase the compactness and strength for gas hydrate-bearing sediments(GHBS), which makes the GHBS exhibiting properties similar to dense sand or cemented soil. Under the frame of unified hardening model of clay and sand (CSUH model), the mechanical properties of GHBS are summarized firstly, and a compressive hardening parameter is introduced to describe the isotropic compression characteristics of GHBS under the double influences of filling and bonding of hydrate. A bonding parameter is put forward to modify the yield function, and an evolution rule of bonding effect is also proposed. The state parameters are used to adjust the dilatancy equation to reflect the dilatancy and softening depending on density. Thus, an elastoplastic model is developed, which can describe the strength, stiffness, shear dilation and strain-softening of GHBS. The model coded and tested, and the simulation results are compared with the experimental ones of GHBS. The results show that the proposed model can well describe the stress-strain relationship, shear contraction with hardening and shear dilation with softening for GHBS.

Keywords: gas hydrate-bearing sediments; compressive hardening; bonding strength; dilatancy; CSUH model

1 Introduction

As a new energy source, gas hydrate (abbreviated as hydrate, commonly known as combustible ice) is widely distributed in the submarine strata. It is regarded as the main clean energy in the 21st century[1] with the advantages of wide distribution, large reserves, high density, and high heating value. The stable existence of hydrates in energy soils (gas hydrate-bearing sediments, GHBS) requires severe temperature and pressure conditions. A little carelessness during drilling and mining may cause a large amount of gas hydrates to decompose. With the decomposition of hydrates, the cementation of soil particles weakens and the porosity increases, and the energy soil becomes under-consolidated soil or loose sand. The decomposed natural gas causes the rapid increase of pore pressure and the decrease of effective stress which leads to the static liquefaction of energy soil resulting in submarine landslide[2]. Submarine landslides seriously threaten the safe mining of combustible ice, destroy hydrate deposits, and even cause the destruction of the submarine ecological environment and the greenhouse effect[2]. Therefore, one of the prerequisites for ensuring the safe mining of combustible ice is to study the mechanical properties of energy soil and construct a reasonable constitutive model for energy soils, and then to solve the strength and deformation problems of submarine energy soil encountered in the mining process from the perspective of geotechnical engineering.

Winters et al.[3] synthesized indoor methane hydrate sand samples by using self-developed high-pressure and low-temperature hydrate triaxial apparatus, and carried out a series of studies such as acoustic wave characteristic test and triaxial shear test, and obtained a preliminary understanding of mechanical properties of energy soil. Masui et al.[4] prepared pore-filled and cemented energy soil samples with two hydrate occurrence modes through different sample preparation methods, and conducted triaxial shear tests. Yun et al.[5] and Wu et al.[6] have also carried out similar material tests on energy soil. The test results show that the content and occurrence mode of hydrate in the energy soil are different, and the mechanical properties are also different. Sultan et al.[7] and Yan et al.[8] analyzed the occurrence modes of hydrates. Based on the experimental research results and analysis, some consensus on the mechanical properties of energy soil was reached: hydrate is filled in the pores of the matrix material which improves the compactness and cohesion of the energy soil and increases the stiffness and strength of energy soil, but has little effect on internal friction angle and Poisson's ratio.

Based on a large number of experimental data, the research on constitutive model of energy soil is also gradually developed. According to the fitting results of test data, Miyazaki et al.[9] defined the expression of tangent modulus related to hydrate saturation (S_h), obtained the tangent Poisson's ratio related to matrix materials by using the least square method, and established a

Received: 18 December 2019 Revised: 08 May 2020
This work was supported by the National Natural Science Foundation of China (11572165, 51778311).
First author: YUAN Qing-meng, male, born in 1988, PhD candidate, mainly engaged in research on marine geotechnics. E-mail: yqm905@126.com
Corresponding author: KONG Liang, male, born in 1969, Professor, Doctoral supervisor, mainly engaged in teaching and research on constitutive modelling of soils and marine geotechnics. E-mail: qdkongliang@163.com

non-linear elastic model of energy soil. However, the volumetric strain was not discussed in the model. Within the framework of critical state soil mechanics, Uchida et al.[10] considered the dilation and cohesiveness of energy soils, and modified the yield surface equation of the modified Cam-clay model (MCC model). The stress-strain relationship and volume deformation relationship of the energy soil were obtained by using the associated flow rule, but it was difficult to determine the hydrate saturation in the mechanical sense through experiments. Sultan et al.[7] analyzed the influence of hydrate on the mechanical properties of energy soil. Starting from the isotropic compression characteristics of energy soil, a constitutive relationship suitable for energy soil was proposed by introducing parameters related to hydrate saturation to modify the hardening law. The comparison between the test and prediction results shows that hydrate provides additional strength for energy soil, and the additional strength gradually declines at the strain-softening stage, so hydrate does not affect the residual strength of energy soil. Li[11] established a new elastic-plastic constitutive model for seabed gas hydrate sediments based on the data obtained from a large number of experimental studies. This model was combined with the secondary loading surface theory and considered the influence of natural gas hydrate on the shear dilation and the cohesion of sediments. Zhang et al.[12] introduced Weibull distribution and residual strength correction coefficient into the damage statistical constitutive model, and established the damage statistical constitutive model of hydrate sediment considering the influence of damage threshold and residual strength. The prediction curve is in good agreement with the test data curve of Masui et al.[4]

From the experimental results of the energy soil and the key research content of constitutive modeling, it can be found that the influence of hydrate on the mechanical properties of energy soil is mainly based on filling and bonding, which makes the energy soil similar to dense sand or cemented soil. To explain and describe the basic characteristics of energy soil, the existing elastoplastic constitutive model can be used after promotion. By introducing appropriate parameters and establishing its evolution law to reflect the filling and bonding effects of hydrate, an elastoplastic constitutive model of energy soil can be established.

Based on the classic MCC model, Yao et al.[13–14] proposed a unified hardening model (UH model) by proposing a unified hardening parameter independent of the stress path. The parameters of UH model are the same as those of MCC model, and can reasonably describe the complex characteristics of special soil, such as shear contraction, dilation, hardening, softening and stress path. In recent years, Yao et al. [15] further proposed a unified hardening model for clays and sands (CSUH model) based on the UH model which not only can describe the over-consolidation characteristics and compactness of clay and sand, but also can regress to UH model and further degenerate into MCC model.

Under the framework of CSUH model, this paper introduces the hardening parameter to describe the influence of hydrate filling and cementation on the compressive strength of energy soil, introduces the cohesive strength to modify the yield function, and uses the state parameters to adjust the dilation equation to reflect the dependence of the dilation and softening characteristics of the energy soil on the compactness. The CSUH model is extended to establish an elastic-plastic constitutive model that can describe the strength, stiffness, dilation and softening of energy soil.

2 Influence of hydrate on mechanical properties of energy soil

Many scholars studied the influence of hydrate on the mechanical properties of energy soil by triaxial tests. Based on different research perspectives, different scholars have different descriptions of the influence mechanism of hydrate [16]. However, regardless of the mechanical mechanism of hydrate affecting the characteristics of energy soil, the filling and bonding effects of hydrate on soil matrix have been generally recognized, that is, the filling and bonding effects of hydrate jointly affect the mechanical properties of energy soil.

This section summarizes the influence of the filling and bonding effects of hydrate on the mechanical behavior of energy soil by analyzing the existing test results, which are mainly manifested in the following aspects:

2.1 Compression characteristic

Compression characteristic is that the modulus of the soil in the compression process increases with the increase in density, that is, the compressive hardening. Figure 1 shows the result of a one-dimensional consolidation test conducted by Kim et al.[17] on energy soils with different hydrate saturation, where S_w is the water content of the sample before preparation which can reflect the size of S_h; σ_v is the vertical stress; and e is the void ratio. It can be seen that:

(1) When σ_v<100 kPa, the void ratio of energy soil is smaller than that of normally consolidated soil which is caused by the filling effect of hydrate on energy soil.

(2) With the increase of σ_v, the compression curve of energy soil is located above the normally consolidated soil, and the curvature is relatively gentle. As S_h increases, the change in void ratio Δe caused by the same stress increment $\Delta\sigma_v$ becomes smaller, and the energy soil exhibits characteristics similar to that of cemented soil or structured soil which reflects the bonding effect of hydrate on the energy soil.

https://rocksoilmech.researchcommons.org/journal/vol41/iss7/5
DOI: 10.16285/j.rsm.2019.7115

(3) When σ_v is greater than a certain pressure, the slope of the compression curve of energy soil increases rapidly, indicating that the bonding effect caused by hydrate begins to decline rapidly. When σ_v is extremely large, the bonding effect of the energy soil is completely lost, and the compression curves are roughly parallel, and the slopes are almost the same.

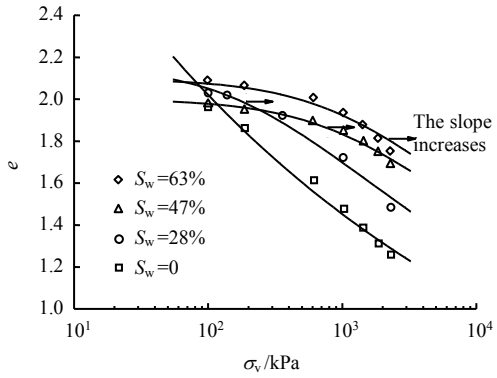

Fig. 1 Effect of S_h on compression characteristics[17]

Since one-dimensional compression and isotropic consolidation have similarities in the methods of description and considering the above-mentioned compression characteristics of energy soil, the compression curve expression proposed by Sheng et al.[18] in the ln$e$-ln$p$ double logarithmic coordinate system is used to describe the normal consolidation line (NCL) of the energy soil:

$$\ln e = \ln N - \lambda \ln\left(p + p_r\right) \tag{1}$$

where λ is the slope of the compression curve, reflecting the shape of NCL; N is the void ratio of energy soil when p+p_r =1 kPa which determines the position of NCL; p is the average principal stress; and p_r is the model parameter which controls the change of the slope of the compression curve.

Figure 2 is the schematic diagram of Eq. (1) in e-ln$p$ space. It can be seen that NCL changes in position and shape with the changes of N and p_r , and when p_r = 0, NCL is approximately a straight line.

It can be seen from Fig. 2 that N and p_r jointly reflect the influence of hydrate on the void ratio of energy soil through Eq. (1), and the change of their values makes the energy soil show the compression characteristics of dense sand, cemented soil or structural soil. The void ratio of the energy soil declines due to the compacting effect of hydrate while the bonding effect allows the energy soil to maintain a larger void ratio. For simplicity, N is expressed as a linear function of S_h:

$$N = N_0 + k_N S_h \tag{2}$$

where k_N is the proportion coefficient that reflects the influence of hydrate on the void ratio of energy soil; and N_0 is the void ratio of the matrix material at p= 1 kPa.

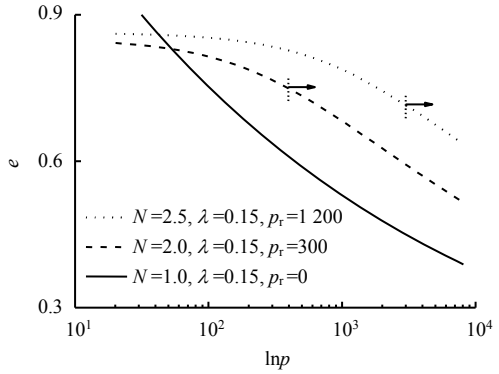

Fig. 2 NCL for GHBS in e–ln$p$ space

To explore the physical meaning of p_r, the curvature K_L of NCL versus ln$p$ is drawn, as shown in Fig. 3. K_L reflects the bending degree of energy soil NCL. It can be seen that K_L has a maximum value when p=p_r, which indicates that the slope of NCL shown in Figs. 1 and 2 begins to increase when p=p_r, and the bonding effect begins to decline. According to the aforementioned analysis of the influence of hydrate filling and bonding effects on the hardening of energy soil, p_r can be defined as the hardening parameter. Combined with the author's previous research foundation[19], the relationship between p_r and S_h satisfies the exponential relationship:

$$p_r = \alpha_r S_h^{\beta_r} \tag{3}$$

where α_r and β_r are model parameters that reflect the influence of hydrate on the hardening of energy soil.

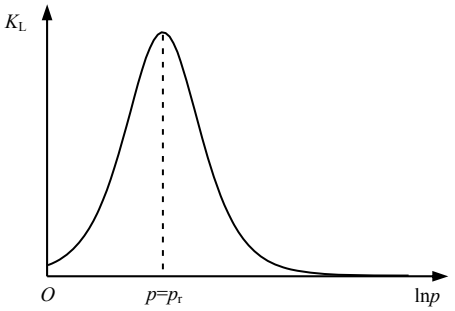

Fig. 3 Relationship between curvature K_L and mean effective stress p

2.2 Friction and cohesive strength

Zhang et al. [20] drew the Mohr's circle of energy soil according to the test results, as shown in Fig.4. σ and τ are principal stress and shear strength while c and φ are cohesion and internal friction angle, respectively. The strength characteristics (i.e. friction) of energy soil in the shear process is different from that of normally consolidated soil. Due to the bonding effect of hydrate on soil skeleton, energy soil has a cohesive force and has higher potential strength. At the same time, it is found that the difference in internal friction angle between energy soil and common soil is not obvious, that is, the internal friction angle remains almost unchanged. Therefore, the potential strength of energy

soil is not only related to the average principal stress p, but also to the cohesion caused by hydrate.

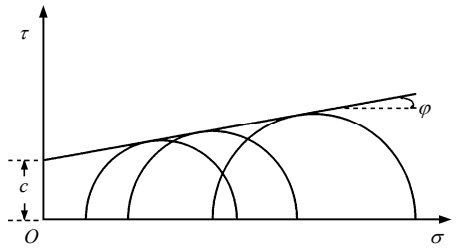

Fig. 4 Schematic plot of Mohr circle of GHBS

Pinkert et al.[21] pointed out that the occurrence form of hydrate is not constant during the deformation process of energy soil. For example, the bonding effect of hydrate increases the strength of energy soil. During the deformation process, the strength is reduced due to the broken cemented structure. At the same time, hydrate particles will be filled in the pore space, thus reducing the void ratio of energy soil, which makes the energy soil behave like dense sand. To reflect the dependence of potential strength of energy soil on hydrate filling and bonding effects, cohesive strength p_t is introduced in this paper based on the description of friction property of normally consolidated soil by MCC model. The critical state line (CSL) of energy soil is described by the following formula:

$$q = M(p + p_t) \tag{4}$$

where M is the critical stress ratio; and q is the deviator stress.

2.3 Stress–strain relationship and shear dilation

Compared with the ordinary soil without hydrate, the energy soil shows some special mechanical properties in the triaxial shear process, as shown in Fig. 5:

(1) The strength of energy soil increases with the increase of effective confining pressure and S_h [3]. As shown in Fig.5, ε_s is the shear strain. When the effective confining pressure is low or S_h is small, the softening of the energy soil is not obvious. As the effective confining pressure or S_h increases, the slope of the initial part of the energy soil stress-strain curve increases gradually, and the peak strength also increases. And the softening phenomenon is gradually obvious after reaching the peak.

(2) The dilation of energy soil is closely related to the effective confining pressure and S_h [4]. As shown in Fig. 5(b), ε_a is the axial strain and ε_v is the volume strain. When S_h is the same, the smaller the effective confining pressure is, the more obvious the dilation of the energy soil is. Under the same effective confining pressure, with the increase of S_h, the dilation of the energy soil increases.

It can be seen from Fig. 5 that under the influence of hydrate filling and bonding effect, the mechanical behavior of energy soil is similar to dense sand, over consolidated soil or cemented soil, and its potential strength changes dynamically during the shearing process.

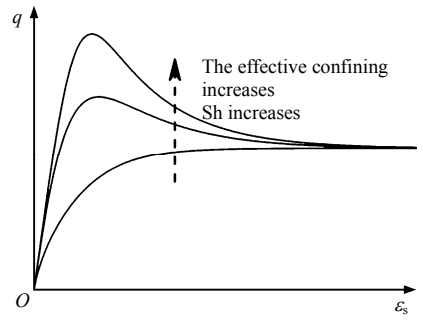

(a) Deviator stress versus axial strain curves of conventional drained triaxial tests

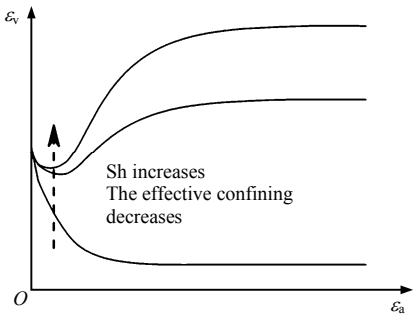

(b) Volumetric strain versus axial strain curves of conventional drained triaxial tests

Fig. 5 Typical schematic plot of mechanical behavior of GHBS

In conclusion, the influence of the filling and bonding effects of hydrate on the mechanical properties of energy soil is mainly manifested in several aspects such as compression characteristics, cohesive strength, stress-strain relationship and dilation, which makes the mechanical properties of the energy soil different from those of normally consolidated soil.

3 Elastoplastic constitutive model of energy soil

3.1 Hardening law

According to Eq. (1), when the consolidation stress increases from p_0 to p_x, the plastic volumetric strain is ε_v^p . p_x and ε_v^p satisfies the relationship:

$$p_x = (p_0 + p_r)\exp\left(\frac{1+e}{\lambda-\kappa}\cdot\frac{\varepsilon_v^p}{e}\right) - p_r \tag{5}$$

where κ is the slope of the unloading curve.

Equation (5) is the hardening law expression obtained from the test of isotropic consolidation compression under a special stress path. It can not reflect the softening and significant dilation characteristics of energy soil strength. Therefore, it can not be directly applied to

the modeling of energy soil.

The hardening parameters of energy soil should be independent of the stress path and contain parameters reflecting potential strength. Yao et al. [15] introduced factors related to the stress path in the CSUH model, and corrected the components related to the stress path in the plastic strain increment, that is, the unified hardening parameter H was used to replace ε_v^p in Eq. (5). The same method is used in this paper:

$$p_x = (p_0 + p_r)\exp\left(\frac{1+e}{\lambda-\kappa}\cdot\frac{H}{e}\right) - p_r \tag{6}$$

H is expressed as:

$$H = \int \frac{1}{R(\eta)}\mathrm{d}\varepsilon_v^p = \int \frac{M_f^4 - \eta^4}{M^4 - \eta^4}\mathrm{d}\varepsilon_v^p \tag{7}$$

where M_f is the potential strength of the energy soil and η is the stress ratio.

3.2 Yield condition

3.2.1 Yield surface function

The yield surface of MCC model is an ellipse with the origin and (p_x, 0) as the two endpoints in p-q coordinate, as shown in the dotted line in Fig. 6, and the expression is shown in the following formula. The CSUH model is modified by introducing a critical state parameter to change the shape of the yield surface. In order to reduce the number of model parameters and simplify the calculation, this paper does not consider the change of yield surface shape. The yield surface expression of MCC model is modified to establish the yield function f of energy soil.

$$f = q^2 + M^2 p(p - p_x) \tag{8}$$

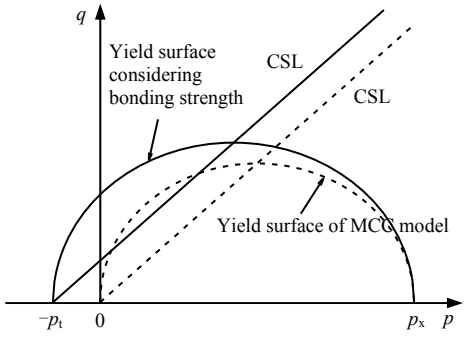

Fig. 6 Schematic diagram of yield surface

As mentioned above, the filling and bonding effects of hydrate jointly improve the potential strength M_f of energy soil, and then affect the compressive strength p_x, as shown in Eq. (6). At the same time, the bonding effect of hydrate makes the energy soil have the tensile strength, and the yield surface equation should reflect this characteristic. Therefore, the cohesive strength p_t of energy soil is introduced so that the yield surface and the negative semi-axis of the p-axis intersect at the point (-p_t, 0). Correspondingly, the CSL line also crosses the point (-p_t, 0), as shown in Eq. (4). The cohesive strength of the energy soil gradually declines during the loading process, and the CSL line gradually shifts to the right and eventually approaches the origin. Based on this, this paper modifies the yield surface equation so that the modified yield surface equation applies to the energy soil:

$$f = q^2 + M^2(p + p_t)(p - p_x) \tag{9}$$

Substituting Eq. (6) into Eq.(9), the yield surface equation with plastic volumetric strain ε_v^p as the hardening parameter is obtained:

$$f = \ln\left(\frac{p+p_t}{p_0+p_r}\right) + \ln\left(\frac{p+p_r}{p+p_t} + \frac{\eta^2}{M^2}\right) - \frac{\varepsilon_v^p}{ec_p} = 0 \tag{10}$$

where the stress ratio η=q/(p+p_t); c_p=($\lambda-\kappa$)/(1+e) which can reflect the plastic stiffness.

The yield surface equation of energy soil can be obtained by substituting ε_v^p in Eq. (10) with the uniform hardening parameter H. Compared with the MCC model, the following formula comprehensively considers the filling and bonding effects of the hydrate.

$$f = \ln\left(\frac{p+p_t}{p_0+p_r}\right) + \ln\left(\frac{p+p_r}{p+p_t} + \frac{\eta^2}{M^2}\right) - \frac{H}{ec_p} = 0 \tag{11}$$

3.2.2 Evolution law of cohesive strength

In the research on cemented soil, most of the existing results assumed that the cohesive strength evolution law is a function of plastic strain. For example, Sun et al.[22] assumed that the cohesive strength is an exponential function of plastic shear strain. Rouainia et al.[23] assumed that it was a function of plastic strain. Suebsuk et al.[24] assumed that the cohesive strength is inversely proportional to the average principal stress p.

According to the method proposed by Uchida et al.[10], this paper assumes that cohesive strength and S_h satisfy the exponential relationship as shown by the following formula:

$$p_t = \alpha_t S_h^{\beta_t} \tag{12}$$

where α_t and β_t are model parameters which can reflect the cohesive strength. When S_h =0, the cohesive strength of normally consolidated soil is 0.

Under the framework of geotechnical elastoplastic theory, the magnitude of the plastic strain increment is represented by the plastic scalar factor Λ. In this paper, combining the research of Zhang[25] and Hu[26], it is assumed that the increment $\mathrm{d}p_t$ is proportional to Λ and is related to the current p_t and p. The evolution law of structural cohesive strength is

$$\mathrm{d}p_t = -(1+e)\frac{ap_t^2}{p}\Lambda \tag{13}$$

where a is a material parameter, which determines the

rate of decline of cohesive strength of energy soil.

The curve of cohesive strength with shear strain under different a is shown in Fig. 7. It can be seen that with the increase of a, the cohesive strength declines faster.

3.3 Flow rule

3.3.1 State parameter and potential strength

The internal state of the sand material is constantly changing during the loading process, and it will eventually become stable. During the deformation process of energy soil, the dilation and compression of the yield surface can reflect the change of the internal state. This change process reflects the evolution process of the potential strength of the energy soil. The CSUH model[15] used the state parameters related to the current void ratio to reflect the dynamic changes of the strength. The state parameter is defined as

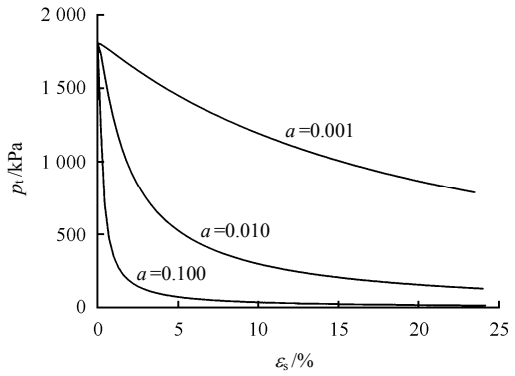

Fig. 7 Evolution of bonding strength with shear strain

$$\xi = e_\eta - e \tag{14}$$

where e_η is the void ratio in the e–ln$p$ space when the stress ratio is η. Combined with Eq. (1), the calculation formula of e_η is

$$e_\eta = \exp\left[\ln(N) - \lambda \ln(p + p_r)\right] - \Delta e_p \tag{15}$$

where Δe_p is the change in void ratio when the stress ratio increases from 0 to η under the path of equal p. Δe_p can be obtained according to Eq. (10):

$$\Delta e_p = e(\lambda - \kappa) \cdot \left[\ln\left(\frac{p + p_t}{p_0 + p_r}\right) + \ln\left(\frac{p + p_r}{p + p_t} + \frac{\eta^2}{M^2}\right)\right] \tag{16}$$

The potential strength M_f can be expressed as a function of state parameters as

$$M_f = M \exp(m\xi) \tag{17}$$

where m is the dilation parameter; and ξ is the state parameter.

3.3.2 Plastic potential function

The expressions of the plastic potential function and yield function are the same when using the associated flow rule:

$$g = \ln\left(\frac{p + p_t}{p_0 + p_r}\right) + \ln\left(\frac{p + p_r}{p + p_t} + \frac{\eta^2}{M^2}\right) - \frac{H}{ec_p} = 0 \tag{18}$$

where g is the plastic potential function.

3.4 Elastoplastic matrix

From Eq. (1), the formula of elastic modulus E of energy soil can be obtained:

$$E = \frac{3(1-2\mu)(1+e)}{\kappa e}(p + p_r) \tag{19}$$

The consistent function of the yield function is

$$\mathrm{d}f = \frac{\partial f}{\partial p}\mathrm{d}p + \frac{\partial f}{\partial q}\mathrm{d}q + \frac{\partial f}{\partial p_t}\mathrm{d}p_t + \frac{\partial f}{\partial H}\mathrm{d}H = 0 \tag{20}$$

Substituting Eqs. (7) and (13) into Eq. (20), the plastic scalar factor is obtained:

$$\Lambda = \frac{1}{\beta}\left(K\frac{\partial f}{\partial p}\mathrm{d}\varepsilon_v + 3G\frac{\partial f}{\partial q}\mathrm{d}\varepsilon_s\right) \tag{21}$$

where

$$\beta = \frac{\partial f}{\partial p}\left(\frac{1}{ec_p R(\eta)} + K\frac{\partial f}{\partial p}\right) + 3G\left(\frac{\partial f}{\partial q}\right)^2 + \frac{\partial f}{\partial p_t}\cdot\frac{a(1+e)p_t^2}{p} \tag{22}$$

where K=E/[3(1−2μ)]; G =E/[2(1+μ)]. K and G are the bulk modulus and shear modulus of energy soil, respectively; and μ is the Poisson's ratio.

The stress-strain relationship in the matrix form is derived as follow:

$$\begin{Bmatrix}\mathrm{d}p\\ \mathrm{d}q\end{Bmatrix} = \begin{bmatrix}D_{pp} & D_{pq}\\ D_{qp} & D_{qq}\end{bmatrix}\begin{Bmatrix}\mathrm{d}\varepsilon_v\\ \mathrm{d}\varepsilon_s\end{Bmatrix} \tag{23}$$

where

$$\left.\begin{aligned} D_{pp} &= K - \frac{K^2}{\beta}\left(\frac{\partial f}{\partial p}\right)^2\\ D_{pq} &= -\frac{3KG}{\beta}\frac{\partial f}{\partial p}\frac{\partial f}{\partial q}\\ D_{qp} &= -\frac{3KG}{\beta}\frac{\partial f}{\partial p}\frac{\partial f}{\partial q}\\ D_{qq} &= 3G - \frac{9G^2}{\beta}\left(\frac{\partial f}{\partial q}\right)^2 \end{aligned}\right\} \tag{24}$$

4 Model prediction

4.1 Model parameters

There are 12 parameters in the model:

(1) λ, κ, μ, M, and m are the physical parameters of Toyoura sand.

(2) N_0, k_N, α_r, and β_r can be determined through consolidation tests of energy soil with different S_h. In addition, the parameters can be obtained by fitting the

initial tangent modulus of energy soil according to Eq. (19) since N_0 and k_N determine the initial void ratio of the energy soil (Eq. (2)), and α_r and β_r determine the compressibility parameter p_r (Eq. (3)).

(3) α_r and β_r can be determined by cohesive strength which is obtained by the common tangent of the Mohr's circle based on the triaxial test data.

(4) a is obtained by fitting the test data of energy soil. Zhang et al.[25] provided the empirical values of a. Considering that the energy soil and its test conditions are different from ordinary soils, a is obtained by fitting the test data in this paper. The decline rates of cohesive strength of energy soil with the same occurrence mode and shear rate are the same. Therefore, when the test results agree with the predicted results well, only a set of test results are needed to determine the parameter a.

4.2 Model prediction

Masui et al. [4] used Toyoura sand and methane gas to prepare energy soil samples with different S_h when the initial void ratio was 0.65. Then triaxial drained tests under an effective confining pressure of 1 MPa were conducted. The proposed model in this paper is used to predict Masui's experimental data, and the parameters are shown in Table 1.

Figure 8 is the prediction result of the energy soil test conducted by Masui et al.[4]. The model prediction fits the experimental data well. The greater the S_h is, the more obvious the filling and bonding effects is, which also leads to a greater corresponding initial stiffness, and a greater corresponding peak strength. After reaching the peak strength, the energy soil gradually tends to the critical state and exhibits strain-softening. Eventually the same residual strength is reached.

Masui et al.[4] gave the volume variation data of the two experiments with S_h =0 and S_h =40.7%. Figure 9 is a comparison diagram of the prediction curve and the experimental data. It can be seen that the model in this paper can describe the shear-induced contraction and dilation of the energy soil. With the increase of S_h, the dilation is more obvious. This is because the larger the S_h is, the more obvious the compaction and bonding effect of energy soil is. On one hand, the occlusive effect between particles is gradually reflected, resulting in the reduction of energy soil shear contraction and even the occurrence of shear dilation. On the other hand, as an additional strength of energy soil, the destruction of cementation structure reduces the cohesive strength of energy soil, which makes the energy soil expand slightly.

To study the mechanical behavior of energy soil under different effective confining pressures, Masui et al. [4] conducted drainage tests on energy soils with similar S_h (34.8%, 34.3%, 33.7%) under effective confining pressures of 1, 2, and 3 MPa. The experimental data are shown as the scatter points in Fig.10. The solid line in the figure is the prediction curve of the model in this paper.

Figure 10 shows that the proposed model can predict the characteristics of energy soil under different effective confining pressures well. It can reflect the characteristics that the strength of energy soil increases with the increase of effective confining pressure. Masui et al. [4] did not provide the volume change data corresponding to Fig.10. In this paper, the volume change data is predicted by using the proposed model, and the prediction curve is shown in Fig. 11. The energy soil first contracts and then dilates rapidly. The dilation becomes more obvious with the decrease of effective confining pressure which means this model can reasonably reflect the dilation of energy soil.

Table 1 Model parameters

λ	κ	μ	M	N_0	k_N	α_r/MPa	β_r	α_t/MPa	β_t	a	m
0.135	0.01	0.3	1.25	2.40	1.21	3.92	0.004	1.02	0.003 1	0.063 7	3.17

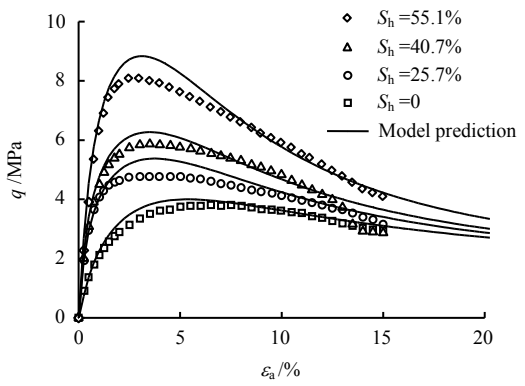

Fig. 8 Comparison between predicted and experimental results for deviator stress versus axial strain [4]

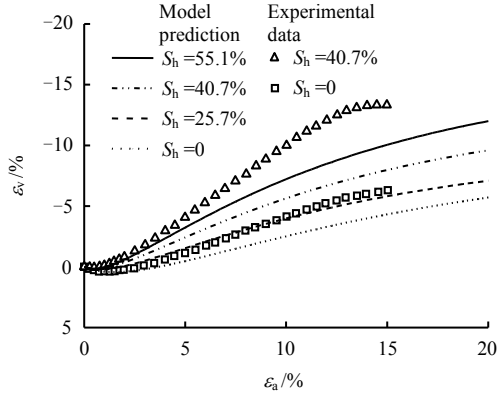

Fig. 9 Comparison between predicted and experimental results for volumetric strain versus axial strain [4]

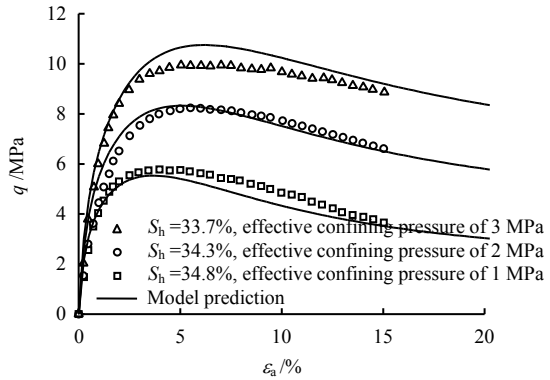

Fig. 10 Comparison between predicted and experimental results for deviatoric stress versus axial strain [4]

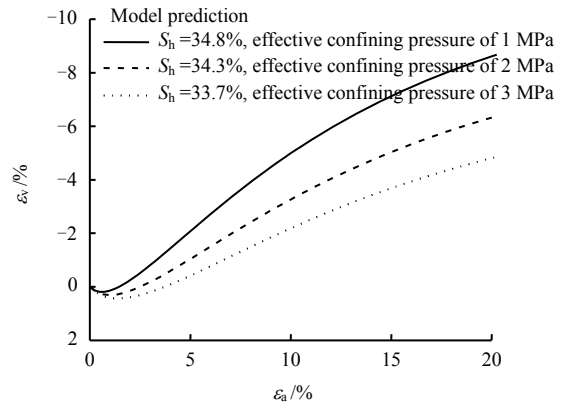

Fig. 11 Predicted volumetric strain versus axial strain

Figures 8–11 show the rationality of the proposed model in this paper. To further verify the applicability of this model, the experimental data by Hyodo et al. [27] are used for comparison. Hyodo et al.[27] used the same sand, preparation method and shear rate as Masui et al.[4]. Therefore, the parameters of the model λ, κ, μ, M, m and a are the same as those in Table 1. Other parameters can be found in Table 2.

Table 2 Model parameters

N_0	k_N	α_r/MPa	β_r	α_t/MPa	β_t
2.9	1.79	45.38	0.246 6	0.1	0

Figure 12 is the comparison diagram of stress-strain behavior between the prediction curve and the test data. It can be seen that the prediction curve is in good agreement with the test data. The model can describe the phenomenon that the initial stiffness of energy soil increases with the increase of S_h, and gradually changes from strain-hardening to strain-softening with the increase of S_h. Since the effective confining pressure in the shear test of energy soil by Hyodo et al.[27] is 5 MPa, which is higher than that of 1 MPa adopted by Masui et al.[4], the model can describe the softening phenomenon of energy soil under lower confining pressure and higher hydrate saturation (Fig. 8 and Fig. 10).

Fig.13 shows the comparison between the prediction and the test data of Hyodo et al.[27]. The model prediction fits the test data well. Compared with the test data of Masui shown in Fig. 9, it can be seen that under high confining pressure, particle breakage and cementation structure failure occur, which then causes the change of volume.

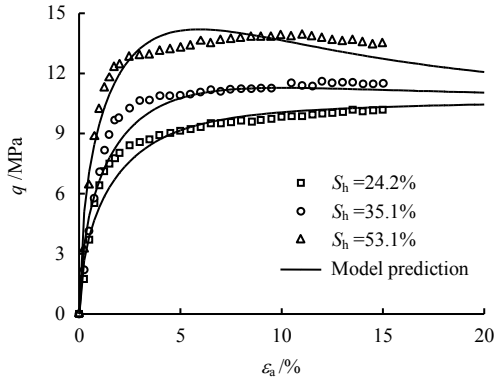

Fig. 12 Comparison between predicted and experimental results for deviator stress versus axial strain [27]

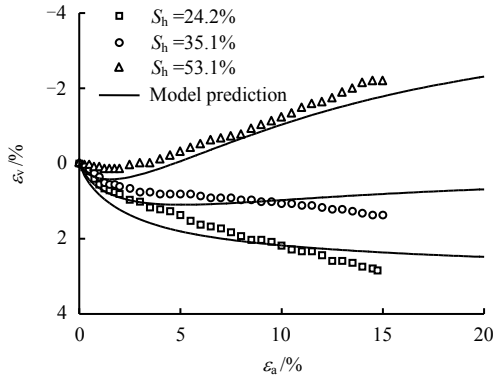

Fig. 13 Comparison between predicted and experimental results for volumetric strain versus axial strain[27]

5 Conclusion

(1) The filling and bonding effects of hydrate affect the mechanical properties of energy soil, which makes the energy soil significantly different from the normally consolidated soil in compression characteristics, cohesive strength, stress-strain relationship and shear dilation.

(2) Under the framework of CSUH model, the parameter N and the compressive hardening parameter p_r are introduced to describe the influence of hydrate on the comprehensive hardening of energy soil. The cohesive strength p_t is introduced and its evolution law is established to reflect the bonding effect of hydrate, and the potential strength of energy soil is reflected by state parameters. The elastoplastic constitutive model of energy soil considering the filling and bonding effects of hydrate is established by using the associated flow rule.

(3) The comparison and analysis of test data and model prediction show that the constitutive model of energy soil has good consistency with test data. This model can describe the characteristics of strain hardening

and softening, strength and stiffness of energy soil.

References

[1] KONG L, ZHANG Z, YUAN Q, et al. Multi-factor sensitivity analysis on the stability of submarine hydrate-bearing slope[J]. China Geology, 2018, 1(3): 367−373.

[2] BROWN H E, HOLBROOK W S, HORNBACH M J, et al. Slide structure and role of gas hydrate at the northern boundary of the Storegga slide, offshore Norway[J]. Marine Geology, 2006, 229(3−4): 179−186.

[3] WINTERS W J, PECHER I A, WAITE W F, et al. Physical properties and rock physics models of sediment containing natural and laboratory-formed methane gas hydrate[J]. American Mineralogist, 2004, 89(8−9): 1221−1227.

[4] MASUI A, HANEDA H, OGATA Y, et al. Effects of methane hydrate formation on shear strength of synthetic methane hydrate sediments[C]//The 15th International Offshore and Polar Engineering Conference. [S. l.]: International Society of Offshore And Polar Engineers, 2005.

[5] YUN T S, SANTAMARINA J C, RUPPEL C. Mechanical properties of sand, silt, and clay containing tetrahydrofuran hydrate[J]. Journal of Geophysical Research: Solid Earth, 2007, 112: B04106.

[6] WU L, GROZIC J L. Laboratory analysis of carbon dioxide hydrate-bearing sands[J]. Journal of Geotechnical and Geoenvironmental Engineering, 2008, 134(4): 547−550.

[7] SULTAN N, GARZIGLIA S. Geomechanical constitutive modelling of gas-hydrate-bearing sediments[C]// Proceedings of the 7th International Conference on Gas Hydrates. Edinburgh: [s. n.], 2011.

[8] YAN Rong-tao, LIANG Wei-yun, WEI Chang-fu, et al. A constitutive model for gas hydrate-bearing sediments considering hydrate occurring habits[J]. Rock and Soil Mechanics, 2017, 38(1): 10−18.

[9] MIYAZAKI K, TENMA N, AOKI K, et al. A nonlinear elastic model for triaxial compressive properties of artificial methane-hydrate-bearing sediment samples[J]. Energies, 2012, 5(10): 4057−4075.

[10] UCHIDA S, SOGA K, YAMAMOTO K. Critical state soil constitutive model for methane hydrate soil[J]. Journal of Geophysical Research: Solid Earth, 2012, 117(B3): 110−116.

[11] LI Yang-hui, Study on strength and deformation behaviors of methane hydrate-Bearing Sediments[D]. Dalian: Dalian University of Technology, 2013.

[12] ZHANG Xiao-ling, XIA Fei, DU Xiu-li, et al. Study on multi-field coupling model considering damage of hydrate-bearing sediments[J]. Rock and Soil Mechanics, 2013, 34(1): 60−65.

[13] YAO Yang-ping, FENG Xing, HUANG Xiang, et al. Application of uh model to finite element analysis[J]. Rock and Soil Mechanics, 2010, 31(1): 237−245.

[14] YAO Yang-ping. Advanced UH models for soils[J]. Chinese Journal of Geotechnical Engineering, 2015, 37(2): 193−217.

[15] YAO Y P, LIU L, LUO T, et al. Unified hardening (UH) model for clays and sands[J]. Computers and Geotechnics, 2019, 110(JUN.): 326−343.

[16] BRUGADA J, CHENG Y P, SOGA K, et al. Discrete element modelling of geomechanical behaviour of methane hydrate soils with pore-filling hydrate distribution[J]. Granular Matter, 2010, 12(5): 517−525.

[17] KIM H S, CHO G C. Experimental study on the compressibility of gas hydrate-bearing sediments[C]//The 2014 World Congress on Advances in Civil, Environmental, and Materials Research. Busan: [s. n.], 2014.

[18] SHENG D C , YAO Y P, CARTER J P. A volume-stress model for sands under isotropic and critical stress states[J]. Canadian Geotechnical Journal, 2015, 45(11): 1639−1645.

[19] YUAN Qing-meng, KONG Liang, LIU Rui-ming, et al. Unified hardening model for gas hydrate bearing sediments considering structure[J]. Science Technology and Engineering, 2018, 18(32): 64−70.

[20] ZHANG Xu-hui, LU Xiao-bing, WANG Shu-yun. Experimental study of static and dynamic properties of tetrahydrofuran hydrate-bearing sediments[J]. Rock and Soil Mechanics, 2011, 32(Suppl. 1): 303−308.

[21] PINKERT S, GROZIC J L H. Failure mechanisms in cemented hydrate-bearing sands[J]. Journal of Chemical and Engineering Data, 2015, 60(2): 376−382.

[22] SUN Kai, CHEN Zheng-lin, LU De-chun. An elastoplastic constitutive model incorporating cementation effect of stabilizer-treated soils[J]. Rock and Soil Mechanics, 2018, 39(5): 1589−1597.

[23] ROUAINIA M, MUIR WOOD D. A kinematic hardening constitutive model for natural clays with loss of structure[J]. Geotechnique, 2000, 50(2): 153−164.

[24] SUEBSUK J, HORPIBULSUK S, LIU M D. A critical state model for overconsolidated structured clays[J]. Computers and Geotechnics, 2011, 38(5): 648−658.

[25] ZHANG feng, YE guan-lin. Computational soil mechanics[M]. Beijing: China Communications Press, 2007.

[26] HU Xiao-rong, DONG Xiao-long, HU Bo-yang, et al. The triple-shear elasto-plastic constitutive model for saturated over-consolidated clay[J]. Chinese Journal of Solid Mechanics, 2017, 38(6): 579−590.

[27] HYODO M, NAKATA Y, YOSHIMOTO N, et al. Challenge for methane hydrate production by geotechnical engineering[J]. Soils and Foundations, 2013, 53(2): 299−314.